Molecular Spinning Top: Visualizing the Dynamics of $M_3N@C_{80}$ with Variable Temperature Single Crystal X-ray Diffraction

Fupin Liu, and Lukas Spree

Electronic Supplementary Information

Experimental Details

Very high-quality single crystals were obtained by co-crystallization of $Ho_2LuN@C_{80}$ or $Lu_3N@C_{80}$ with NiOEP. X-ray diffraction data collection was carried out at the BESSY storage ring (BL14.3, Berlin-Adlershof, Germany).[1] XDSAPP2.0 suite was employed for data processing.[2] The structure was solved by direct methods and refined by SHELXL-2018.[3] Hydrogen atoms were added geometrically, and refined with a riding model. The crystal data are presented in Table S1 and S5 in the ESI.

Table S1. Crystal data_$Ho_2LuN@C_{80}$.

Crystal	$Ho_2LuN@C_{80}$⊃NiOEP⊃2(C_6H_6)	$Ho_2LuN@C_{80}$⊃NiOEP⊃2(C_6H_6)	$Ho_2LuN@C_{80}$⊃NiOEP⊃2(C_6H_6)
Formula	C_{128} H_{56} Ho_2 Lu N_5 Ni	C_{128} H_{56} Ho_2 Lu N_5 Ni	C_{128} H_{56} Ho_2 Lu N_5 Ni
Formula weight	2227.31	2227.31	2227.31
Color, habit	Black, block	Black, block	Black, block
Crystal system	triclinic	triclinic	triclinic
Space group	$P\bar{1}$	$P\bar{1}$	$P\bar{1}$
***a*, Å**	14.700(3)	14.730(3)	14.750(3)
***b*, Å**	15.380(3)	15.410(3)	15.430(3)
***c*, Å**	17.730(4)	17.740(4)	17.760(4)
***α*, deg**	81.00(3)	81.10(3)	81.21(3)
***β*, deg**	74.53(3)	74.48(3)	74.41(3)
***γ*, deg**	86.56(3)	86.55(3)	86.49(3)
Volume, Å³	3815.0(15)	3832.5(15)	3846.7(15)
Z	2	2	2
***T*, K**	100	130	160
Radiation (λ, Å)	Synchrotron Radiation (0.89429)	Synchrotron Radiation (0.89429)	Synchrotron Radiation (0.89429)
Unique data (R_{int})	14968 (0.0418)	15130 (0.0474)	14943 (0.0485)
Parameters	1268	1288	1311
Restraints	43	51	105
Observed data ($I > 2\sigma(I)$)	13648	13210	12158
R_1[a] (observed data)	0.0504	0.0629	0.0728
wR_2[b] (all data)	0.1459	0.1820	0.2193
CCDC NO.	1947203	1947204	1947205

[a]For data with $I > 2\sigma(I)$, $R_1 = \frac{\sum||F_o| - |F_c||}{\sum|F_o|}$. [b]For all data, $wR_2 = \sqrt{\frac{\sum\left[w\left(F_o^2 - F_c^2\right)^2\right]}{\sum\left[w\left(F_o^2\right)^2\right]}}$.

Table S1. Crystal data_$Ho_2LuN@C_{80}$_continued.

Crystal	$Ho_2LuN@C_{80}$□NiOEP□2(C_6H_6)	$Ho_2LuN@C_{80}$□NiOEP□2(C_6H_6)	$Ho_2LuN@C_{80}$□NiOEP□2(C_6H_6)
Formula	C_{128} H_{56} Ho_2 Lu N_5 Ni	C_{128} H_{56} Ho_2 Lu N_5 Ni	C_{128} H_{56} Ho_2 Lu N_5 Ni
Formula weight	2227.31	2227.31	2227.31
Color, habit	Black, block	Black, block	Black, block
Crystal system	triclinic	triclinic	triclinic
Space group	$P\bar{1}$	$P\bar{1}$	$P\bar{1}$
***a*, Å**	14.760(3)	14.800(3)	14.810(3)
***b*, Å**	15.460(3)	15.490(3)	15.500(3)
***c*, Å**	17.790(4)	17.890(4)	17.940(4)
***α*, deg**	81.26(3)	81.20(3)	81.15(3)
***β*, deg**	74.34(3)	74.06(3)	73.94(3)
***γ*, deg**	86.42(3)	86.21(3)	86.15(3)
Volume, Å^3	3862.4(15)	3895.9(15)	3909.1(15)
Z	2	2	2
***T*, K**	190	250	280
Radiation (λ, Å)	Synchrotron Radiation (0.89429)	Synchrotron Radiation (0.89429)	Synchrotron Radiation (0.89429)
Unique data (R_{int})	11923 (0.0541)	15398 (0.0571)	15466 (0.0613)
Parameters	1321	1321	1309
Restraints	825	1102	1210
Observed data ($I > 2\sigma(I)$)	9856	10717	10338
R_1[a] (observed data)	0.0808	0.1304	0.1462
wR_2[b] (all data)	0.2372	0.4232	0.4549
CCDC NO.	1947206	1947207	1947208

[a]For data with $I > 2\sigma(I)$, $R_1 = \frac{\sum||F_o| - |F_c||}{\sum|F_o|}$. [b]For all data, $wR_2 = \sqrt{\frac{\sum\left[w\left(F_o^2 - F_c^2\right)^2\right]}{\sum\left[w\left(F_o^2\right)^2\right]}}$.

Table S2. Nearest cage carbon-Ni contact distances as a function of temperature_$Ho_2LuN@C_{80}$

Temperature (K)	100	130	160	190	250	280
Ni1P-C1A (Å)	2.810(6)	2.812(7)	2.795(8)	2.81(1)	2.85(2)	2.86(2)

Table S3. Selected M-N bond lengths as a function of temperature_$Ho_2LuN@C_{80}$

Temperature (K)	100	130	160	190	250	280
Ho1-N1 (Å)	2.050(4)	2.058(4)	2.063(4)	2.047(5)	2.032(6)	2.020(6)
Ho2-N1 (Å)	2.043(4)	2.036(4)	2.016(4)	2.007(5)	2.018(6)	1.998(7)
Ho3-N1 (Å)	2.018(5)	2.019(6)	2.026(5)	2.025(6)	2.028(8)	2.039(9)
Ho4-N1 (Å)	2.052(4)	2.043(5)	2.022(4)	2.005(5)	2.032(5)	1.999(7)
Ho5-N1 (Å)	1.96(2)	1.99(2)	1.978(7)	1.96(1)	1.98(1)	1.94(1)
Ho6-N1 (Å)		2.018(9)	2.011(6)	2.00(1)	1.977(8)	1.973(9)
Ho7-N1 (Å)		2.053(9)	2.037(6)	2.015(7)	2.012(7)	1.986(8)
Ho8-N1 (Å)		1.98(2)	1.98(2)	1.96(2)	1.92(2)	1.94(2)
Ho9-N1 (Å)			1.99(2)	2.01(2)	2.00(2)	2.02(2)
Ho10-N1 (Å)				1.99(2)	2.01(1)	2.00(1)
Ho11-N1 (Å)				2.01(2)	2.02(2)	1.99(2)
Average (Å)	**2.044(5)**	**2.039(6)**	**2.025(6)**	**2.011(7)**	**2.010(8)**	**1.993(9)**
Lu1-N1 (Å)	2.042(4)	2.033(4)	2.013(5)	2.071(6)	2.003(8)	1.930(7)
Lu2-N1 (Å)	2.055(5)	2.025(5)	1.978(5)	1.970(7)	1.922(7)	1.957(9)
Lu3-N1 (Å)		2.031(6)	2.075(6)	1.932(7)	1.954(7)	2.026(7)
Average (Å)	**2.044(5)**	**2.031(5)**	**2.014(5)**	**1.992(7)**	**1.956(8)**	**1.984(8)**
Ni1P-N1P (Å)	1.968(4)	1.964(4)	1.963(4)	1.961(5)	1.949(6)	1.958(6)
Ni1P-N2P (Å)	1.962(3)	1.967(4)	1.964(4)	1.966(4)	1.963(5)	1.961(5)
Ni1P-N3P (Å)	1.968(4)	1.970(4)	1.968(4)	1.966(5)	1.957(5)	1.965(6)
Ni1P-N4P (Å)	1.969(3)	1.970(4)	1.970(4)	1.964(4)	1.973(5)	1.979(5)
Average (Å)	**1.967(4)**	**1.968(4)**	**1.966(4)**	**1.964(5)**	**1.960(6)**	**1.966(6)**

Table S4. Metal site occupancy in $Ho_2LuN@C_{80}$ as a function of temperatures

Metal sites	100K	130K	160K	190K	250K	280K
Lu1	0.8370(11)	0.6459(13)	0.4505(16)	0.3510(17)	0.2625(17)	0.2289(17)
Ho1	0.8370(11)	0.6459(13)	0.4505(16)	0.3510(17)	0.2625(17)	0.2289(17)
Ho2	0.8370(11)	0.6459(13)	0.4505(16)	0.3510(17)	0.2625(17)	0.2289(17)
Lu2	0.1630(11)	0.2592(12)	0.3346(14)	0.3120(17)	0.3171(17)	0.2775(18)
Ho3	0.1630(11)	0.2592(12)	0.3346(14)	0.3120(17)	0.3171(17)	0.2775(18)
Ho4	0.1407(15)	0.2592(12)	0.3346(14)	0.3120(17)	0.3171(17)	0.2775(18)
Lu3		0.0949(13)	0.2147(16)	0.3369(19)	0.420(2)	0.493(2)
Ho5	0.0223(13)	0.0652(14)	0.1520(18)	0.205(2)	0.210(3)	0.225(3)
Ho6		0.0441(13)	0.0793(15)	0.116(2)	0.157(3)	0.169(3)
Ho7		0.0298(12)	0.0629(14)	0.097(2)	0.144(2)	0.183(3)
Ho8		0.0509(16)	0.0629(18)	0.092(2)	0.114(3)	0.132(3)
Ho9			0.0727(19)	0.075(2)	0.086(2)	0.095(2)
Ho10				0.0352(17)	0.067(2)	0.085(2)
Ho11				0.055(2)	0.063(3)	0.098(3)

Table S5. Crystal data_$Lu_3N@C_{80}$.

Crystal	$Lu_3N@C_{80}$□NiOEP□2(C_6H_6)	$Lu_3N@C_{80}$□NiOEP□2(C_6H_6)	$Lu_3N@C_{80}$□NiOEP□2(C_6H_6)
Formula	C_{128} H_{56} Lu_3 N_5 Ni	C_{128} H_{56} Lu_3 N_5 Ni	C_{128} H_{56} Lu_3 N_5 Ni
Formula weight	2247.39	2247.39	2247.39
Color, habit	Black, block	Black, block	Black, block
Crystal system	triclinic	triclinic	triclinic
Space group	$P\bar{1}$	$P\bar{1}$	$P\bar{1}$
***a*, Å**	14.700(3)	14.750(3)	14.780(3)
***b*, Å**	15.380(3)	15.440(3)	15.480(3)
***c*, Å**	17.730(4)	17.770(4)	17.860(4)
***α*, deg**	81.04(3)	81.20(3)	81.20(3)
***β*, deg**	74.47(3)	74.32(3)	74.11(3)
***γ*, deg**	86.42(3)	86.38(3)	86.20(3)
Volume, Å^3	3814.1(15)	3849.5(15)	3882.6(15)
Z	2	2	2
***T*, K**	100	160	220
Radiation (λ, Å)	Synchrotron Radiation (0.89429)	Synchrotron Radiation (0.89429)	Synchrotron Radiation (0.89429)
Unique data (R_{int})	9532 (0.1360)	13109 (0.1523)	10914 (0.1745)
Parameters	1263	1327	1320
Restraints	1020	897	1165
Observed data ($I > 2\sigma(I)$)	7538	8161	6459
R_1[a] (observed data)	0.0673	0.1212	0.1576
wR_2[b] (all data)	0.2075	0.4062	0.4704
CCDC NO.	1947140	1947141	1947142

[a]For data with $I > 2\sigma(I)$, $R_1 = \frac{\sum||F_o| - |F_c||}{\sum|F_o|}$. [b]For all data, $wR_2 = \sqrt{\frac{\sum\left[w\left(F_o^2 - F_c^2\right)^2\right]}{\sum\left[w\left(F_o^2\right)^2\right]}}$.

Table S5. Crystal data_$Lu_3N@C_{80}$_continued.

Crystal	$Lu_3N@C_{80}$□NiOEP□2(C_6H_6)
Formula	C_{128} H_{56} Lu_3 N_5 Ni
Formula weight	2247.39
Color, habit	Black, block
Crystal system	triclinic
Space group	$P\bar{1}$
***a*, Å**	14.820(3)
***b*, Å**	15.500(3)
***c*, Å**	17.960(4)
***α*, deg**	81.11(3)
***β*, deg**	73.86(3)
***γ*, deg**	86.07(3)
Volume, Å³	3914.0(15)
Z	2
***T*, K**	280
Radiation (λ, Å)	Synchrotron Radiation (0.89429)
Unique data (R_{int})	12095 (0.2152)
Parameters	1320
Restraints	1309
Observed data ($I > 2\sigma(I)$)	6204
R_1[a] (observed data)	0.1605
wR_2[b] (all data)	0.4542
CCDC NO.	1947143

[a]For data with $I > 2\sigma(I)$, $R_1 = \frac{\sum||F_o| - |F_c||}{\sum|F_o|}$. [b]For all data, $wR_2 = \sqrt{\frac{\sum\left[w\left(F_o^2 - F_c^2\right)^2\right]}{\sum\left[w\left(F_o^2\right)^2\right]}}$.

Table S6. Nearest cage carbon-Ni contact distances as a function of temperature_$Lu_3N@C_{80}$

Temperature (K)	100	160	220	280
Ni1P-C1A (Å)	2.79(2)	2.83(1)	2.83(3)	2.83(2)

Table S7. Selected M-N bond lengths as a function of temperature_$Lu_3N@C_{80}$

Temperature (K)	100	160	220	280
Lu1A-N1 (Å)	2.022(8)	2.019(10)	2.088(13)	2.157(14)
Lu2A-N1 (Å)	2.072(8)	1.990(9)	2.027(10)	2.007(10)
Lu3A-N1 (Å)	2.048(8)	2.101(8)	2.019(11)	1.976(11)
Lu1B-N1 (Å)	1.998(10)	2.023(11)	2.057(13)	2.051(13)
Lu2B-N1 (Å)	2.071(10)	2.013(9)	2.049(11)	2.019(9)
Lu3B-N1 (Å)	1.996(9)	2.053(9)	2.028(13)	2.010(12)
Lu1C-N1 (Å)		1.94(2)	1.98(2)	1.93(2)
Lu2C-N1 (Å)		2.00(2)	1.96(2)	1.935(14)
Lu3C-N1 (Å)		2.06(2)	1.91(2)	1.90(2)
Lu1D-N1 (Å)		1.93(2)	1.88(2)	1.90(2)
Lu2D-N1 (Å)		1.97(2)	1.96(2)	1.979(12)
Lu3D-N1 (Å)		2.028(13)	1.95(2)	1.91(2)
Lu2F-N1 (Å)		2.02(2)	1.95(3)	1.92(2)
Lu3E-N1 (Å)		2.04(3)	1.97(3)	1.96(2)
Lu3F-N1(Å)			2.00(3)	1.96(2)
Average (Å)	**2.044(9)**	**2.02(2)**	**2.00(2)**	**1.98(2)**
Ni1P-N1P (Å)	1.974(7)	1.969(8)	1.949(9)	1.965(8)
Ni1P-N2P (Å)	1.973(9)	1.961(10)	1.938(10)	1.961(9)
Ni1P-N3P (Å)	1.972(7)	1.968(8)	1.946(9)	1.967(8)
Ni1P-N4P (Å)	1.950(9)	1.941(10)	1.982(10)	1.944(9)
Average (Å)	**1.967(8)**	**1.960(9)**	**1.954(10)**	**1.959(9)**

Table S8. Metal site occupancy in $Lu_3N@C_{80}$ as a function of temperatures

Metal sites	100K	160K	220K	280K
Lu1A	0.853(2)	0.5127(18)	0.3104(19)	0.2407(18)
Lu2A	0.853(2)	0.5127(18)	0.3104(19)	0.2407(18)
Lu3A	0.853(2)	0.5127(18)	0.3104(19)	0.2407(18)
Lu1B	0.147(2)	0.2610(17)	0.2812(19)	0.2819(18)
Lu2B	0.147(2)	0.2610(17)	0.2812(19)	0.2819(18)
Lu3B	0.147(2)	0.2610(17)	0.2812(19)	0.2819(18)
Lu1C		0.075(2)	0.141(3)	0.153(3)
Lu2C		0.117(3)	0.210(3)	0.202(3)
Lu3C		0.078(2)	0.111(3)	0.130(3)
Lu1D		0.151(2)	0.267(3)	0.324(3)
Lu2D		0.075(2)	0.127(3)	0.194(3)
Lu3D		0.085(2)	0.104(3)	0.125(3)
Lu2F		0.034(2)	0.071(3)	0.081(3)
Lu3E		0.063(2)	0.093(3)	0.104(3)
Lu3F			0.100(3)	0.118(3)

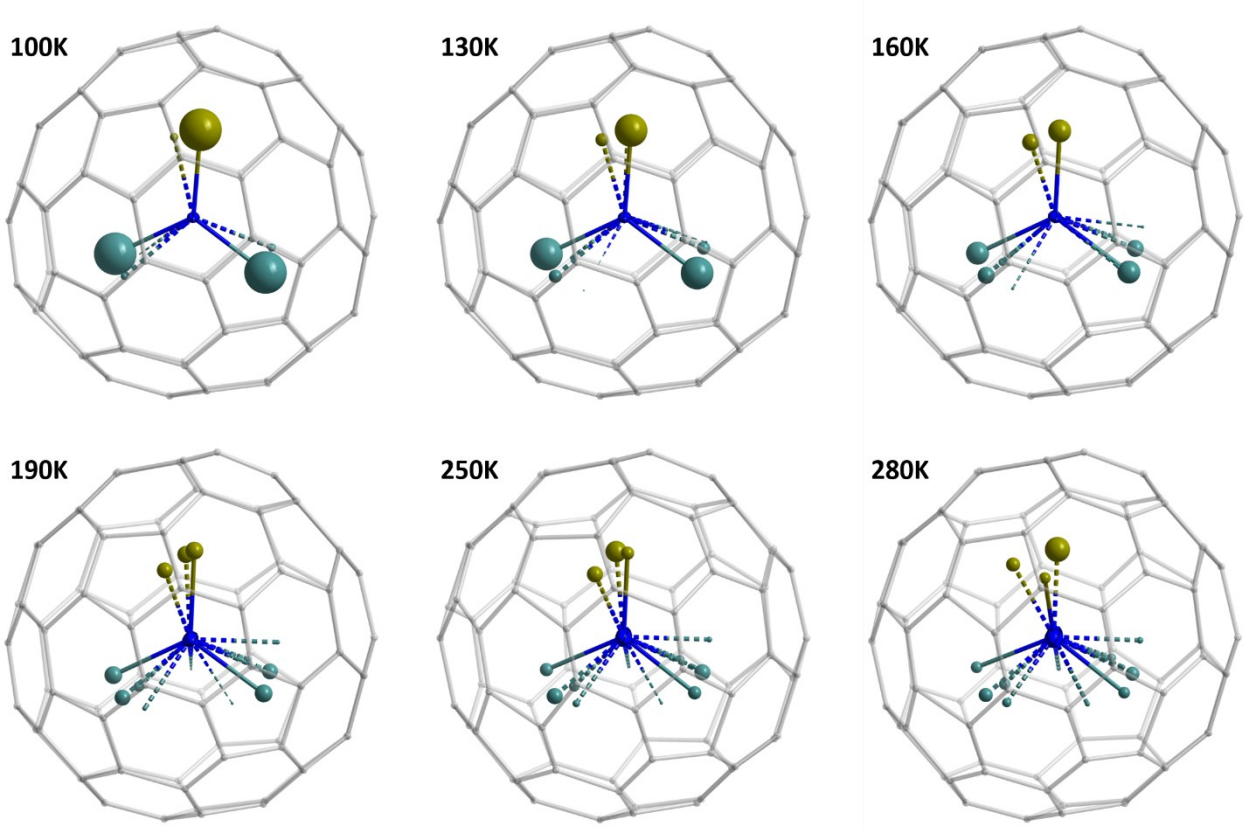

Fig. S1. Molecular structure of $Ho_2LuN@C_{80}$·NiOEP·2(C_6H_6) measured with single-crystal X-ray diffraction at variable temperatures from 100K to 280K. The metal sites are shown as spheres whose radii are scaling proportional to the site occupancy (the bigger the sphere, the higher the occupancy). Color code: grey for carbon, brown for Lu, cyan for Ho, and blue for N.

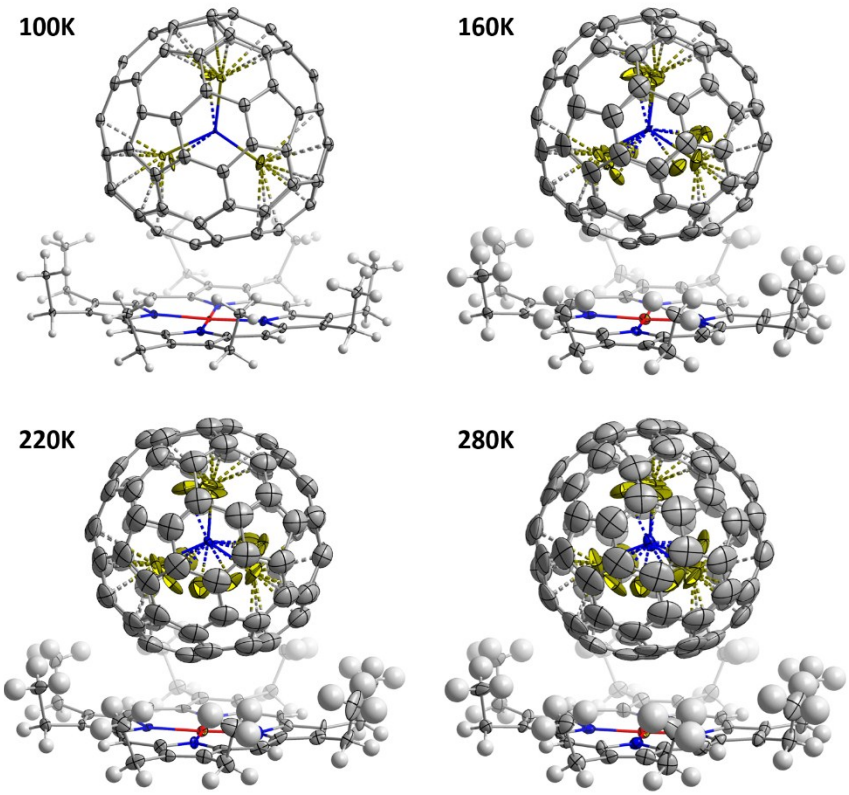

Fig. S2. Single-crystal X-ray structures of $Lu_3N@C_{80}$·NiOEP·2(C_6H_6) measured at variable temperatures from 100K to 280K. Solvent molecules are omitted for clarity. The displacement parameters are shown at the 30% probability level. The structures are drawn from a specific direction of the crystal to easily compare the dynamics of the $Lu_3N@C_{80}$. Color code: grey for carbon, brown for Lu, blue for N, white for H, and red for Ni.

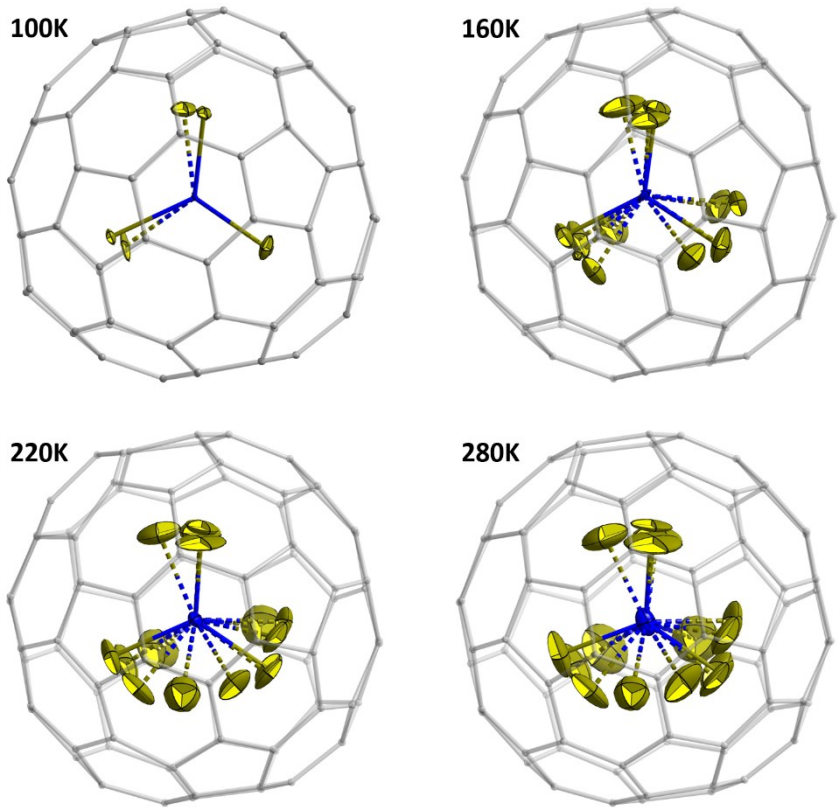

Fig. S3. Molecular structures of $Lu_3N@C_{80}$·NiOEP·2(C_6H_6) measured with single crystal X-ray diffraction at variable temperatures from 100K to 280K. NiOEP and solvent molecules are omitted for clarity. The displacement parameters are shown at the 30% probability level for the encapsulated Lu_3N cluster. The structures are drawn from the chosen specific direction of the crystal to compare the dynamics of the Lu_3N @C_{80}. Color code: grey for carbon, brown for Lu, and blue for N.

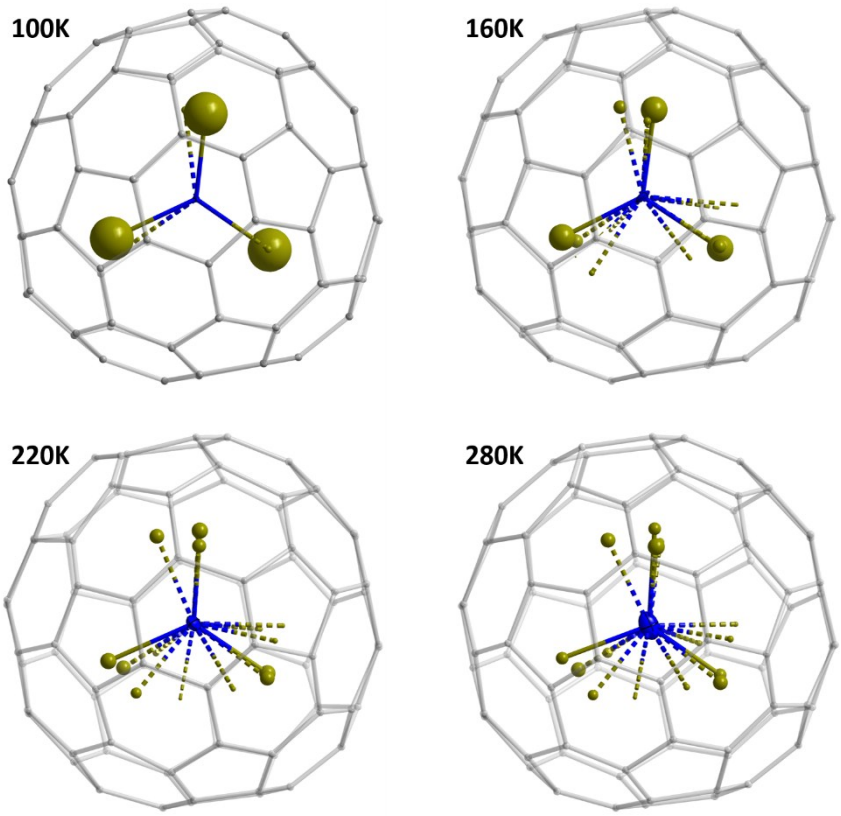

Fig. S4. Molecular structure of $Lu_3N@C_{80}$·NiOEP·2(C_6H_6) measured with single-crystal X-ray diffraction at variable temperatures from 100K to 280K. The metal sites are shown as spheres whose radii are scaling proportional to the site occupancy (the bigger the sphere, the higher the occupancy). Color code: grey for carbon, brown for Lu, and blue for N.

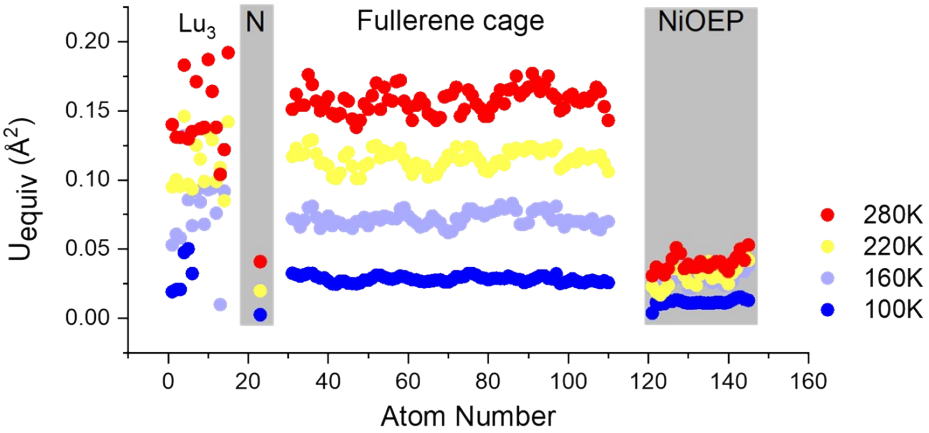

Fig. S5. Equivalent atomic displacement parameters of $Lu_3N@C_{80}$·NiOEP·2(C_6H_6) as a function of temperature between 100 and 280K. The encapsulated N and co-crystallized NiOEP were highlighted with grey rectangles.

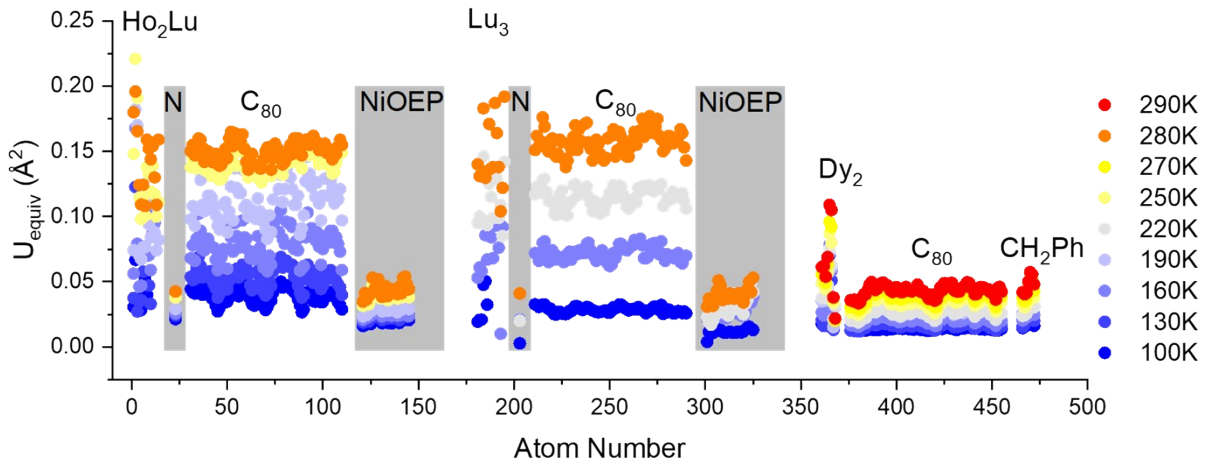

Fig. S6. Comparison of equivalent atomic displacement parameters of $Ho_2LuN@C_{80}$·NiOEP·2(C_6H_6), $Lu_3N@C_{80}$·NiOEP·2(C_6H_6), and $Dy_2@C_{80}$-CH_2Ph·0.67(C_7H_8)[4] as a function of temperature between 100 and 290K. The encapsulated N and co-crystallized NiOEP were highlighted with grey rectangles.

Reference:

1. U. Mueller, R. Förster, M. Hellmig, F. U. Huschmann, A. Kastner, P. Malecki, S. Pühringer, M. Röwer, K. Sparta, M. Steffien, M. Ühlein, P. Wilk and M. S. Weiss, *Eur. Phys. J. Plus*, 2015, **130**, 141.
2. K. M. Sparta, M. Krug, U. Heinemann, U. Mueller and M. S. Weiss, *J. Appl. Cryst.*, 2016, **49**, 1085-1092.
3. G. Sheldrick, *Acta Cryst. C*, 2015, **71**, 3-8.
4. (a) F. Liu, G. Velkos, D. S. Krylov, L. Spree, M. Zalibera, R. Ray, N. A. Samoylova, C.-H. Chen, M. Rosenkranz, S. Schiemenz, F. Ziegs, K. Nenkov, A. Kostanyan, T. Greber, A. U. B. Wolter, M. Richter, B. Büchner, S. M. Avdoshenko and A. A. Popov, *Nat. Commun.*, 2019, **10**, 571; (b) F. Liu, D. S. Krylov, L. Spree, S. M. Avdoshenko, N. A. Samoylova, M. Rosenkranz, A. Kostanyan, T. Greber, A. U. B. Wolter, B. Büchner and A. A. Popov, *Nat. Commun.*, 2017, **8**, 16098.